Least Square Method for the Identification of Equivalent Inertia Constant

Muyang Liu*, Junru Chen*, Yongsheng Xie†, Xiaoyu Deng* and Federico Milano§
* School of Electrical Engineering, Xinjiang University, Urumqi, China
{muyang.liu, junru.chen}@xju.edu.cn
† State Grid Xinjiang Electric Power Co., LTD, China
§ School of Electrical & Electronic Engineering, University College Dublin, Ireland
federico.milano@ucd.ie

***Abstract*—This paper proposes a simple yet accurate least square method to identify the equivalent inertia constant of individual inertia providers. The proposed method requires ambient measurements and is based on the well-known classical swing equation of synchronous machines. The proposed method shows a very good accuracy for the inertia identification of the rotational and virtual inertia in different operating conditions, including stationary ones, and can also be used to quantify the inertia support effect of the time-varying adaptive inertia.**

***Index Terms*—Inertia constant identification, frequency control, frequency stability, virtual inertia.**

I. Introduction

A. Motivation

The ongoing move from Synchronous Generator (SG) to Inverter-Based resources (IBRs) is expected to reduce the ability of the system to cope with frequency variations and, in effect, power unbalances, due to the loss of the rotational inertia [1]. In this context, a variety of virtual inertia control schemes has been developed to enforce the IBR to mimic the SG mechanism for the purpose of providing a fast frequency support and emulating the inertial support of SG [2].

The concept "equivalent inertia constant" is used to quantify the ability of the inertia response from both the SG and IBR to counteract the variation of the Rate of Change of Frequency (RoCoF) in the system [3]. This kind of control is incentivized by market mechanisms that are currently under discussion by Transmission System Operators (TSOs) around the world. For example, the Chinese government has recently announced that the "inertia market" should be developed along with the IBRs-leading power system. This inertia market includes both rotational [4] and virtual inertia [5] and may contribute to improve the system stability, as well as reduce carbon emissions. This paper tackle precisely this identification problem and proposes a simple yet highly reliable method to estimate the equivalent inertia constant based on measurements currently available to TSOs.

B. Literature Review

In order to form an efficient inertia market and properly reward the inertia provision by IBRs, TSOs will need a method to accurately detect and identify the equivalent inertia constant of the devices connected to the grid. A variety of on-line inertia identification approaches has been proposed in recent years [6]–[9]. These methods are based on the assumption of the availability of Phasor Measurement Units (PMUs) data, which are currently widely utilized by TSOs. These approaches, however, require the occurrence of events that trigger a significant variation of the frequency at the nodes of the grid. Another feature of these methods is that they focus on obtaining a fast estimation but, depending on the transient, they might not be accurate.

On the other hand, the inertia market is more likely to require accurate inertia information of each IBR under different operating conditions, rather than instantaneous estimations of their inertial response. In this vein, [10]–[13] propose inertia identification approaches based on ambient measurement data and recursive techniques by introducing hypothesis models of the inertia provider. The accuracy of these approaches, however, highly rely on the accuracy with which the parameters of the model of the device under estimation. These parameters need to be tuned case by case. With this aim, various techniques including modal analysis [10], [11], dynamic regressor extension [12] and variable-order polynomial fitting [13], have been proposed.

C. Contribution

This paper proposes an ambient measurement data-driven inertia identification method based on the Rate of Change of Power (RoCoP) estimation technique provided in [9], [14], [15]. The proposed approach has two advantages: (i) it works for a variety of operating conditions, including stationary ones; and (ii) it is independent from the device and, in fact, it can be used to quantify the virtual inertial response of non-synchronous devices. This technique, thus, appears to potentially fit better future inertia market than the existing methods.

D. Organization

The remainder of the paper is organized as follows. Section II reviews the concept of the equivalent inertia constant and the existing inertia identification formula provided in [9], [14]. Section III proposes a least square method for inertia constant identification based on ambient measurement data. Section IV validates the proposed method for both rotational and virtual inertia for various scenarios. Finally, conclusions are drawn in Section V.

II. Estimation of Equivalent Inertia Constant

A. Rotational Inertia

Rotational inertia is a property of the SGs, which store kinetic energy through their rotating shafts. This kinetic energy is naturally utilized by synchronous machine to compensate power imbalances. The well-known swing equation [16] describing the motion of SGs originally defines the equivalent inertia constant, in per unit, is as follows:

$$M_{\mathrm{SG}}\,\dot{\omega}_{\mathrm{SG}} = p_{m,\mathrm{SG}} - p_{e,\mathrm{SG}} - p_{D,\mathrm{SG}}\ , \tag{1}$$

where ω_{SG} is the angular frequency of the synchronous machine, $p_{m,\mathrm{SG}}$ and $p_{e,\mathrm{SG}}$ are the mechanical and electrical power; $p_{D,\mathrm{SG}}$ is the active power variation due to damping effect, and:

$$p_{D,\mathrm{SG}} = D_{\mathrm{SG}}(\omega_{\mathrm{Grid}} - \omega_{\mathrm{SG}}) \tag{2}$$

where D_{SG} is the damping coefficient; and M_{SG} is the mechanical starting time of SGs and is measured in seconds. $D_{\mathrm{SG}} \ll M_{\mathrm{SG}}$ always holds for synchronous machines. The starting time M_{SG} is linked to the inertia constant of the machine, as follows:

$$M_{\mathrm{SG}} = 2H_{\mathrm{RI}} = \frac{J_{\mathrm{RI}}\,\omega_{n,\mathrm{SG}}^2}{S_{n,\mathrm{SG}}}\ , \tag{3}$$

where H_{RI} is the equivalent inertia constant, J_{RI} is the rotational inertia, and ω_n and S_n are the nominal angular frequency and the nominal power, respectively, of the SG.

In (1), $p_{e,\mathrm{SG}}$ can be measured directly; ω_{SG} can be accurately estimated through the bus frequency measured by PMUs [17]; while for all kinds of inertia provider, p_m can not be measured directly and the estimation approach is also missing. Therefore, to solve H_{RI} through (1), one has to cope with the effect of p_m and $p_{D,\mathrm{SG}}$. References [9], [14] provide an elegant solution by firstly splitting the p_m into three components:

$$p_m = p_{\mathrm{UC}} + p_{\mathrm{PFC}} + p_{\mathrm{SFC}}\ , \tag{4}$$

where p_{UC} is the power set point obtained by solving the unit commitment problem; p_{PFC} and p_{SFC} are the active power regulated by the Primary Frequency Control (PFC) and Secondary Frequency Control (SFC) correspondingly.

Then, differentiating (1) and substituting (4), one obtains:

$$2H_{\mathrm{RI}}\,\ddot{\omega}_{\mathrm{SG}} = \dot{p}_{\mathrm{UC}} + \dot{p}_{\mathrm{PFC}} + \dot{p}_{\mathrm{SFC}} - \dot{p}_{e,\mathrm{SG}} + \dot{p}_{D,\mathrm{SG}}\ , \tag{5}$$

where $\dot{p}_e$, abbreviated as RoCoP, can be estimated through PMUs measurements [18], [19]; the time derivative of RoCoF, namely $\ddot{\omega}$, can be obtained through the PMUs measurements with a PI filter [9].

In (5), $\dot{p}_{\mathrm{UC}} = 0$, $\dot{p}_{\mathrm{SFC}} \approx 0$ and $\dot{p}_{D,\mathrm{SG}} \ll \dot{p}_{e,\mathrm{SG}}$, $\dot{p}_{\mathrm{PFC}} \ll \dot{p}_{e,\mathrm{SG}}$ always hold within the period between the rescheduling of generations, i.e., in the time window that characterizes the inertial response of the generator. Thus, for proper time window, one can expect that:

$$2H_{\mathrm{RI}} \approx -\frac{\dot{p}_{e,\mathrm{SG}}}{\ddot{\omega}_{\mathrm{SG}}}\ . \tag{6}$$

A detail discussion about the time window for inertia identification is provided in Section III-A.

B. Virtual Inertia

The implementation of controllers able to provided virtual inertial support through IBRs has been under intense investigation in recent years. Provided that the IBR has an active power reserve, the "virtual inertia" is a control scheme that mimics the SG transients on the frequency support:

$$p_{e,\mathrm{IBR}} = p_{\mathrm{UC}} + p_{\mathrm{PFC}} + p_{\mathrm{SFC}} + p_{\mathrm{VI}} - p_{D,IBR}, \tag{7}$$

where p_{VI} is the power boosted by the virtual inertia:

$$p_{\mathrm{VI}} = -2H_{\mathrm{VI}}\dot{\omega}_{\mathrm{IBR}}\ . \tag{8}$$

Equations (7)-(8) indicates that H_{VI} can also be estimated through (6). Since the virtual inertial support is the results of a control action, H_{VI} can be adaptively tuned, through proper measurements of system states, in order to better counteract with the frequency deviations following a contingency [20]. With this regard, the on-line inertia estimation approach proposed in [9] can track the time-varying adaptive H_{VI}. For inertia markets, however, an "equivalent inertia constant" should be defined to price the inertia support of the time-varying inertia. The proposed technique presented in Section III provides a potential solution to identify the equivalent constant of the adaptive virtual inertia, as discussed in Section II-B.

III. Least Square Inertia Constant Identification

A. Time window for inertia identification

Figure 1 shows a typical frequency dynamic behavior of a power system with high IBR penetration.

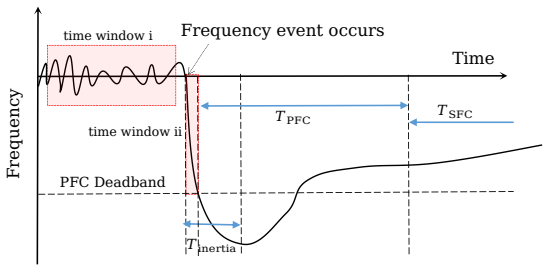

Fig. 1. Frequency dynamics of a power system with high IBR penetrations.

In Fig. 1, T_{inertia} indicates the inertial response period following a frequency event; T_{PFC} and T_{SFC} are the time scales of PFC and SFC; and the red rectangles are the suitable time windows for the identification of inertia through the formula (9). The rationales behind these time windows are the following.

1) Normal operating condition with continuously small disturbance: In practice, power systems are continuously subject to small disturbances arising from the stochastic variations of loads and renewable IBRs [21]. In normal operating conditions, the power system suppresses these stochastic dynamics mainly through the filtering effect of the inertial response

of synchronous machines. In this scenario, since frequency deviations are within the deadband of the frequency control, $\dot{p}_{\mathrm{SFC}} = \dot{p}_{\mathrm{PFC}} = 0$ holds. Moreover, the time window utilized in the propsed estimation of the inertia is long enough to make the proposed estimation robust with respect to ambient noise and other fast fluctuations.

2) Inertial response period following a frequency events within the deadband of PFC: This time window is characterized by relatively large $\ddot{\omega}$ and $\dot{p}_e$ and, thus, the impact of measurement noise on the inertia identification can be mitigated compared to the normal operating condition. Figure 1 shows that the inertial response and conventional PFC period are partly overlapped. However, the time scale of PFC, especially that procided by non-synchronous devices, cannot be defined exactly as there exist both slow, fast and very fast PFCs. As a rule of thumb, the estimation time window has to be long enough to carry out an accurate inertia identification, while short enough to avoid the impact of conventional PFC. Fast PFCs will likely overlap with the estimation, thus being accounted for as "virtual inertia." Finally, very fast PFC will be filtered out by the windowing technique.

Note also that we assume that the estimation time window is shorter than the dispatch period of the generators. In any case, the TSO is aware of when generation dispatch changes occur and, thus, they can discard the estimations at those times.

B. Problems of Existing Formula

Equation (6) indicates that the equivalent inertia constant can be identified through the ambient measurements of the inertia provider. In practical applications and when considering real-world data, the inertia estimation formula (6) needs to be modified to cope with measurement errors. With this aim, (6) can be rewritten as:

$$2H^* = -\frac{\dot{p}^*}{\ddot{\omega}^*} = -\frac{\dot{p}_e + \xi_p}{\ddot{\omega} + \xi_\omega}\,, \tag{9}$$

where the superscript $*$ denotes the measured/estimated value and ξ indicates measurement errors.

While mathematically correct, (9) cannot be applied as is. The following are relevant numerical and practical issues:

- When $\ddot{\omega}^* \to 0$ (notably, in quasi-steady-state conditions), the effect ξ_p will be dramatically amplified through the infinitesimal denominator, and result in a severe error in the estimation of M^*.
- The conditions $\dot{p}_{\mathrm{PFC}} \ll \dot{p}_e$ and $\dot{p}_{\mathrm{D}} \ll \dot{p}_e$ might not be always satisfied. This is, in particular, an issue for selecting the time window locating following a frequency event.

C. Data-based Least Square Method

This subsection presents the proposed Least Square Method (LSM) for the inertia identification based on (9) and proper time-windowing of the measurements, which is implemented to mitigate the potential estimation discussed in subsection III-A.

According to (9), for the measurement data obtained at time t_i, one has:

$$H \approx H_i^* = \frac{|\dot{p}^*(t_i)|}{2|\ddot{\omega}^*(t_i)|}\,, \tag{10}$$

where the absolute values of $\dot{p}^*$ and $\ddot{\omega}^*$ are considered for simplicity but without loss of the relevant information.

It is convenient to rewrite (10) as:

$$2|\ddot{\omega}^*(t_i)|\, H_i^* - |\dot{p}^*(t_i)| \approx 0\,. \tag{11}$$

For a set of measurements $t_1, t_2, \ldots, t_{N-1}, t_N$, one can define the following vectors:

$$\boldsymbol{A} = 2[|\ddot{\omega}^*(t_1)|,\, |\ddot{\omega}^*(t_2)|,\, \ldots,\, |\ddot{\omega}^*(t_{N-1}|),\, \ddot{\omega}^*(t_N)]^T$$
$$\boldsymbol{b} = [|\dot{p}^*(t_1)|,\, |\dot{p}^*(t_2)|,\, \ldots,\, |\dot{p}^*(t_{N-1})|,\, |\dot{p}^*(t_N)|]^T\,,$$

where ^{T} denotes the matrix transposition; $\boldsymbol{A}$ and $\boldsymbol{b}$ are the matrices consisting of the data $\ddot{\omega}^*$ and $\dot{p}^*$ collected within the time window $[t_1, t_N]$, the data size N of each matrix is decided by the length of the time window $\tau = t_N - t_1$ and the sampling rate of the PMU.

We propose the following LSM to find M^*:

$$\text{Minimize } (\boldsymbol{A}H^* - \boldsymbol{b})^2\,, \tag{12}$$

which admits the well-known solution:

$$H^* = (\boldsymbol{A}^T\boldsymbol{A})^{-1}\boldsymbol{A}^T\boldsymbol{b}\,. \tag{13}$$

Equation (13) is the sought expression to identify the equivalent inertia constant. Note that to avoid ill-conditioned $\boldsymbol{A}^T\boldsymbol{A}$, it is convenient to condition its diagonal elements with small diagonal elements. In the test that have been solved when preparing this work, we have utilized $\epsilon = 10^{-6}$ to prevent $\boldsymbol{A}^T\boldsymbol{A}$ to be singular.

The proposed LSM can mitigate the impact of the issues discussed in Section III-B by properly selecting the time window during which the measurements of $\ddot{\omega}^*$ and $\dot{p}^*$ are collected. To further reduce numerical issues, in the case study presented below, we filter the measurement data by removing all pairs $(|\ddot{\omega}^*|, |\dot{p}^*|)$ for which $|\ddot{\omega}^*| < 10^{-5}$ pu(Hz)/s^2 and the 2% the most extreme outliers.

It is important to note that the proposed technique, unlike the on-line inertia estimation method proposed in [9] that can track the time-varying inertia, is expected to return an "average" value of the equivalent inertia constant within a given time window.

IV. Case Study

This section validates the proposed LSM technique with a modified version of the WSCC 9-bus system [16]. The SGs connected at bus 1 and 3 are replaced by a virtual inertia provider, i.e., a Virtual Synchronous Generator (VSG), and a Wind Power Plant (WPP) that provides little inertia to the system, as shown in Fig. 2. The modified system has a 75.6% non-synchronous power generation.

The bus frequency and the output active power of each inertia provider are measured with PMUs with sampling rate

50 Hz. The $\ddot{\omega}^*$ and $\dot{p}^*$ are obtained using the technique based on PI filters that is described in [9]. All simulations presented in this case study were obtained using the Python-based software tool Dome [22].

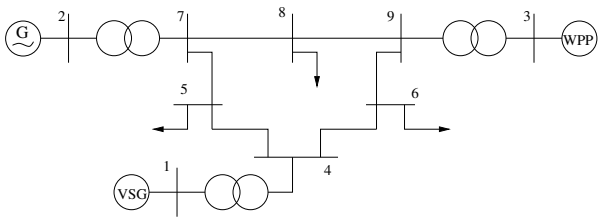

Fig. 2. Modified WSCC 9-bus system.

A. Identification of Rotational Inertia

The SG has $H_{\mathrm{SG}} = 23.64$ MWs/MVA, $D_{\mathrm{SG}} = 1.0$ MW/MVA. In this subsection, noise is modeled as an Ornstein-Uhlenbeck stochastic process and is added to each measurements [23]. The dynamic wind speed of the WPP is modeled as a Weibull distribution with exponentially decaying autocorrelation [24].

In normal operating conditions, the power system is affected by continutous wind and load fluctuations. For illustration, Fig. 3 shows the trajectories $\ddot{\omega}^*$ and $\dot{p}^*$ for a 10 s time window. These are obtained assuming the knowledge of H_{RI}. This figures indicates, qualitatively at least, that the assumptions made to obtain equation (9) are well satisfied in this scenario.

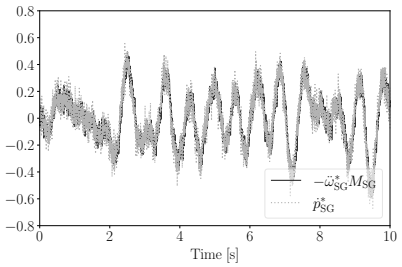

Fig. 3. Dynamic trajectories of SG of the modified WSCC 9-bus system in normal operating conditions.

The equivalent inertia constant identification results of the SG with different length of the time window (recorded as T) are shown in Fig. 4. According to this figure, the proposed inertia identification technique is relatively accurate in normal operating conditions for time windows above 3 s, with the relative error distributed in the range $[0.7, 2.51]$ %.

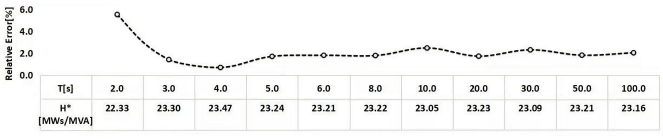

T[s]	2.0	3.0	4.0	5.0	6.0	8.0	10.0	20.0	30.0	50.0	100.0
H* [MWs/MVA]	22.33	23.30	23.47	23.24	23.21	23.22	23.05	23.23	23.09	23.21	23.16

Fig. 4. Equivalent inertia constant identification results for the SG in normal operating conditions.

Next, we consider the transient response of the modified WSCC 9-bus system following a large disturbance, namely a sudden load increase at bus 5, occurring at $t = 0.1$ s. The transient behavior of the SG following the disturbance are shown in Fig. 5.

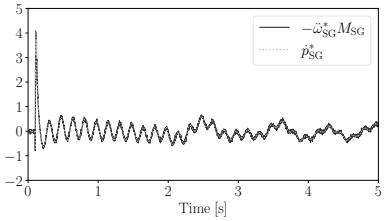

Fig. 5. Trajectories of the SG of the modified WSCC 9-bus system following a sudden load increase.

Figure 6 shows the results of the proposed inertia identification for the SG for different time windows following the occurrence of the disturbance. The time windows with length $\in [0.3, 15]$ s are long enough to identify the equivalent inertia constant of the SG through the proposed LSM with satisfied accuracy, namely relative error smaller than 1%. Figure 5 also indicates that the effect of the measurement noise are less evident compared to the normal operating condition scenario shown in Fig. 3, and thus the accuracy of inertia identification increases.

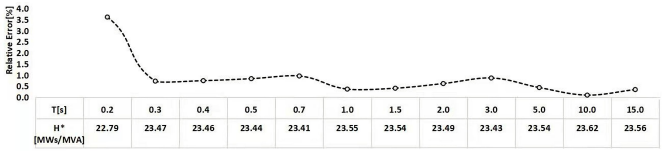

T[s]	0.2	0.3	0.4	0.5	0.7	1.0	1.5	2.0	3.0	5.0	10.0	15.0
H* [MWs/MVA]	22.79	23.47	23.46	23.44	23.41	23.55	23.54	23.49	23.43	23.54	23.62	23.56

Fig. 6. Equivalent inertia constant identification results for the SG following a sudden load increase.

B. Virtual Inertia Identification

In this section, we consider the inertia identification of the VSG at Bus 1 with different virtual inertia techniques, namely the constant virtual inertia control discussed in [2] and the adaptive virtual inertia control discussed in [20]. Note that, since the accuracy of the proposed LSM has been validated in the example discussed in Section IV-A, this section focuses on presenting the inertia identification of the time-varying inertia. For simplicity, noise is not considered in the simulations discussed below.

For constant virtual inertia, $H_{\mathrm{VI}} = 20$ MWs/MVA, the adaptive virtual inertia has the same H_{VI} during the normal operating condition and varies corresponding to the RoCoF following frequency events. The plots of Fig. 7 show the trajectories of the VSG following the sudden load increase. The adaptive inertia allows extra support with the constant inertia control and slightly improves the overall frequency response of the system.

Figure 8 shows the results for the identification of constant and adaptive virtual inertia within the 15 s time window following the occurrence of a sudden load increase. For constant

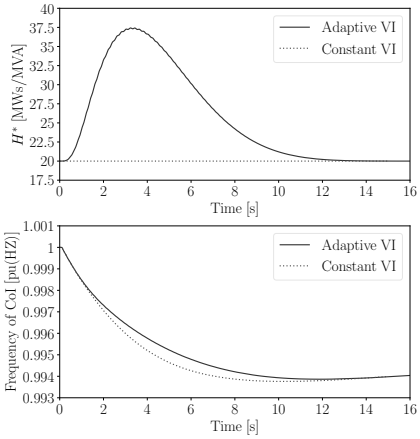

Fig. 7. Trajectories of the modified WSCC 9-bus system with different virtual inertia provider. Upper panel: trajectories of H^*_{VI}, lower panel: trajectories of the frequency of CoI.

inertia, the LSM returns $H^*_{\text{constant,VI}} = 20.02$ MWs/MVA, which has a relative error of only 0.1%. The right panel of Fig. 8 shows that all data pairs are distributed closely to the $H^*_{\text{constant,VI}}$. On the other hand, for adaptive inertia, the distributions of the data pairs are more scattered and the $H^*_{\text{adaptive,VI}} = 23.9$ MWs/MVA. The $H^*_{\text{adaptive,VI}}$ is 19.3% bigger than $H^*_{\text{constant,VI}}$. These results indicate that the proposed technique can be used to quantify the extra inertia support from the adaptive technique.

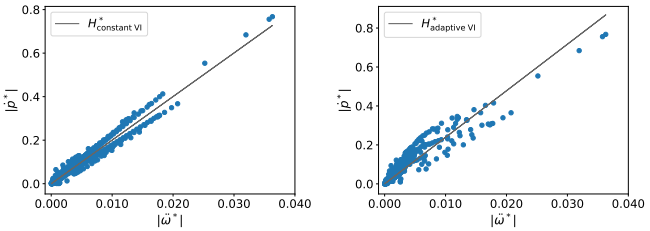

Fig. 8. LSM-based inertia identification results for the VSG with different virtual inertia techniques.

V. Conclusions

This paper proposes an LSM problem that builds on top of the inertia estimation formulas presented in [14] and is able to solve the numerical issues that affect such techniques. The proposed approach is adequate for the estimation of the equivalent inertia of both rotating machines and virtual inertia providers through ambient measurement data. Simulation results show that the proposed inertia identification approach has a high accuracy for time windows of the order of 1 s under various operating conditions, including stationary normal operation. The proposed technique can also be utilized to quantify the "average" inertia support from a time-varying inertia control. Thus, the proposed approach appears as an useful tool to provide information on the availability of inertia for the coming inertia market. Future work will aim at improving the LSM-based estimation using, for example, Tikhonov's or Lassos' methods.

References

[1] F. Milano, F. Dörfler, G. Hug, D. J. Hill, and G. Verbič, "Foundations and challenges of low-inertia systems," in *PSCC*, 2018, pp. 1–25.

[2] S. D'Arco, J. A. Suul, and O. B. Fosso, "A virtual synchronous machine implementation for distributed control of power converters in smartgrids," *EPSR*, vol. 122, pp. 180 – 197, 2015.

[3] R. K. Panda, A. Mohapatra, and S. C. Srivastava, "Application of indirect adaptive control philosophy for inertia estimation," in *IEEE PES GTD Grand Int. Conf. and Exp. Asia*, 2019, pp. 478–483.

[4] W. Li, P. Du, and N. Lu, "Design of a new primary frequency control market for hosting frequency response reserve offers from both generators and loads," *IEEE Trans. on Smart Grid*, vol. 9, no. 5, pp. 4883–4892, 2018.

[5] B. K. Poolla, S. Bolognani, N. Li, and F. Dörfler, "A market mechanism for virtual inertia," *IEEE Trans. on Smart Grid*, vol. 11, no. 4, pp. 3570–3579, 2020.

[6] R. K. Panda, A. Mohapatra, and S. C. Srivastava, "Online estimation of system inertia in a power network utilizing synchrophasor measurements," *IEEE Trans. on Power Systems*, pp. 1–1, 2019.

[7] J. Schiffer, P. Aristidou, and R. Ortega, "Online estimation of power system inertia using dynamic regressor extension and mixing," *IEEE Trans. on Power Systems*, vol. 34, no. 6, pp. 4993–5001, 2019.

[8] J. Zhang and H. Xu, "Online identification of power system equivalent inertia constant," *IEEE Trans. on Industrial Electronics*, vol. 64, no. 10, pp. 8098–8107, 2017.

[9] M. Liu, J. Chen, and F. Milano, "On-line inertia estimation for synchronous and non-synchronous devices," *IEEE Trans. on Power Systems*, vol. 36, no. 3, pp. 2693–2701, 2021.

[10] Y. Wehbe, L. Fan, and Z. Miao, "Least squares based estimation of synchronous generator states and parameters with phasor measurement units," in *North American Power Symposium (NAPS)*, 2012, pp. 1–6.

[11] P. Makolo, R. Zamora, and T.-T. Lie, "Online inertia estimation for power systems with high penetration of res using recursive parameters estimation," *IET Ren. Power Gen.*, vol. 15, p. 2571–2585, 2021.

[12] J. Schiffer, P. Aristidou, and R. Ortega, "Online estimation of power system inertia using dynamic regressor extension and mixing," *IEEE Trans. on Power Systems*, vol. 34, no. 6, pp. 4993–5001, 2019.

[13] C. Phurailatpam, Z. H. Rather, B. Bahrani, and S. Doolla, "Measurement-based estimation of inertia in ac microgrids," *IEEE Trans. on Sustainable Energy*, vol. 11, no. 3, pp. 1975–1984, 2020.

[14] F. Milano and Á. Ortega, "A method for evaluating frequency regulation in an electrical grid – Part I: Theory," *IEEE Trans. on Power Systems*, vol. 36, no. 1, pp. 183–193, 2021.

[15] Á. Ortega and F. Milano, "A method for evaluating frequency regulation in an electrical grid – Part II: Applications to non-synchronous devices," *IEEE Trans. on Power Systems*, vol. 36, no. 1, pp. 194–203, 2021.

[16] P. Sauer and M. Pai, *Power System Dynamics and Stability*. Prentice Hall, 1998.

[17] F. Milano, Á. Ortega, and A. J. Conejo, "Model-agnostic linear estimation of generator rotor speeds based on phasor measurement units," *IEEE Trans. on Power Systems*, pp. 1–1, 2018.

[18] F. Teng, M. Aunedi, D. Pudjianto, and G. Strbac, "Benefits of demand-side response in providing frequency response service in the future Gb power system," *Frontiers in Energy Research*, vol. 3, p. 36, 2015.

[19] T. Kerdphol, F. S. Rahman, M. Watanabe, Y. Mitani, D. Turschner, and H. Beck, "Enhanced virtual inertia control based on derivative technique to emulate simultaneous inertia and damping properties for microgrid frequency regulation," *IEEE Access*, vol. 7, pp. 14 422–14 433, 2019.

[20] J. Chen, M. Liu, F. Milano, and T. O'Donnell, "Adaptive virtual synchronous generator considering converter and storage capacity limits," *IEEE Trans. on Power Systems*, 2020.

[21] M. A. A. Murad, F. M. Mele, and F. Milano, "On the impact of stochastic loads and wind generation on under load tap changers," in *IEEE PES General Meeting*, 2018, pp. 1–5.

[22] F. Milano, "A Python-based software tool for power system analysis," in *IEEE PES General Meeting*, Vancouver, BC, Jul. 2013.

[23] F. Milano and R. Zárate-Miñano, "A systematic method to model power systems as stochastic differential algebraic equations," *IEEE Trans. on Power Systems*, vol. 28, no. 4, pp. 4537–4544, 2013.

[24] R. Zárate-Miñano and F. Milano, "Construction of SDE-based wind speed models with exponentially decaying autocorrelation," *Renewable Energy*, vol. 94, no. C, pp. 186–196, 2016.